

Thermodynamics of Crew-Cut Micelle Formation of Polystyrene-*b*-Poly(acrylic acid) Diblock Copolymers in DMF/H₂O Mixtures

Hongwei Shen, Lifeng Zhang, and Adi Eisenberg*

Department of Chemistry, McGill University, 801 Sherbrooke Street West, Montreal, Quebec, Canada H3A 2K6

Received: January 7, 1997; In Final Form: March 26, 1997[⊗]

The thermodynamics of formation of “crew-cut” micelles of polystyrene-*block*-poly(acrylic acid) (PS-*b*-PAA) diblock copolymers were investigated. The PAA/PS ratios were in the range 0.08–0.33, and *N,N*-dimethylformamide/water (DMF/H₂O) mixtures were used as the selective solvent. For the block ratios investigated here, the copolymers form spherical crew-cut micelles with a large PS core and a thin PAA corona. The temperature dependence of the critical micelle concentration (cmc) was determined under different conditions from scattered light intensity measurements as a function of temperature. The closed association model was found to describe the micellization process and was used to calculate the standard Gibbs free energies (ΔG°), the standard enthalpies (ΔH°), and the standard entropies (ΔS°). The effects of solvent composition, copolymer composition, and added NaCl content on the thermodynamic functions were studied. From the experimental data, a single set of combined equations for the standard thermodynamic functions was obtained. These are the following: ΔG°_{298K} (kJ mol⁻¹) = 20.4 – 0.00859 N_{PS} + 0.00938 N_{PAA} – 10.2 W_{H_2O} – 3.65 mM_{NaCl} ; ΔH° (kJ mol⁻¹) = –151 + 0.0906 N_{PS} – 0.0692 N_{PAA} + 7.38 W_{H_2O} – 22.9 mM_{NaCl} ; ΔS° (J mol⁻¹ K⁻¹) = –574 + 0.333 N_{PS} – 0.264 N_{PAA} + 59.0 W_{H_2O} – 64.5 mM_{NaCl} . N_{PS} and N_{PAA} are the block lengths of the two copolymer components; W_{H_2O} is the weight percent of water in DMF; mM_{NaCl} is the millimolar concentration of NaCl. ΔG° , ΔH° , and ΔS° values were all found to be negative under experimental conditions, which indicates that the standard entropy is unfavorable and that the standard enthalpy is solely responsible for micelle formation. However, it was also found that the enthalpy-driven process could be transformed to an entropy-driven process by increasing the water content or increasing the PS block length. The effect of homopolystyrene on the light scattering behavior during micellization was also studied. It was found that the addition of homopolystyrene increased the critical micelle temperatures (cmts) significantly.

1. Introduction

The self-assembly of block copolymers to micelles in selective solvents, which thermodynamically favor one of the blocks, has been of great interest for several decades.^{1–3} Because of their composition, amphiphilic copolymers in aqueous media can form regular micelles with a hydrophobic core and a hydrophilic corona, or reverse micelles in organic solvents. Both regular and reverse micelles, which have been studied to date, generally have a small core and a relatively long corona and are frequently referred to as star-like micelles. Micelles of another type, i.e., “crew-cut” micelles, which are characterized by a large core and a relatively short corona, have been receiving attention only recently.^{4–12} This type of micelle structure was first foreseen by de Gennes,¹³ and Halperin et al. introduced the name “crew-cut”.¹⁴

Recently, we reported the results of a series of investigations of crew-cut micelle-like aggregates formed from polystyrene-*b*-poly(acrylic acid) (PS-*b*-PAA) copolymers composed of long PS blocks and relatively short PAA blocks.^{5–9} It was found that the core radii are not only dependent on the insoluble block lengths but are also affected by the lengths of the soluble blocks.⁵ Furthermore, it was found that aggregates of multiple morphologies can be formed in low molecular weight solvents by varying the composition of the block copolymers, the polymer concentration, the common solvent, and the type and concentration of added ions such as HCl, CaCl₂, and NaOH.^{6–8,12}

The aggregates were prepared by dissolving the copolymers in DMF or DMF/water mixtures,¹¹ adding deionized water dropwise until ca. 25 wt % of deionized water had been added to the mixtures, and finally dialyzing the mixtures against distilled water.⁶ In view of all these investigations, we believe that a study of the thermodynamics of micellization, initially for spherical micelles, should improve our understanding the system.

In the investigations of the thermodynamics of block copolymer micellization, difficulties can arise due to rate effects, in contrast to micelle formation of small molecule surfactants, which is generally very fast. For the crew-cut system in which the cores have a high glass transition temperature (T_g is ca. 100 °C for polystyrene), equilibrium may be unattainable over reasonable time scales. On the other hand, the solvent, which is present in the micelle cores, acts as a plasticizer and thus increases the exchange rate at which unassociated chains and micelles are able to reach thermodynamic equilibrium. Therefore, the presence of solvent and its concentration in the micelle cores are important factors for reaching thermodynamic equilibrium.

There are mainly two experimental approaches for studying the thermodynamics of copolymer micellization. One involves using the closed-association model to estimate the standard thermodynamic functions based on measurements of the critical micelle concentration (cmc) or the critical micelle temperature (cmt). The other involves a direct enthalpy measurement by techniques such as differential scanning calorimetry (DSC). The first approach is the one most frequently used and may involve the use of static light scattering (SLS),^{15–26} UV–visible spectroscopy,^{27–29} fluorescence spectroscopy,^{29,30} DSC tech-

* To whom correspondence should be addressed. E-mail: eisenber@omc.lan.mcgill.ca.

[⊗] Abstract published in *Advance ACS Abstracts*, May 1, 1997.

niques,³¹ and many others.^{1,32} Among all these techniques, SLS is the most popular way to investigate the thermodynamics by monitoring the temperature-induced micellization process. The DSC approach, in general, cannot give the standard enthalpy directly but only the enthalpy under experimental conditions.^{32–34}

The thermodynamics of micellization have been investigated for several copolymer systems. Price and co-workers studied polystyrene-*b*-poly(ethylene/propylene) (PS-*b*-PEP) and polystyrene-*b*-polyisoprene (PS-*b*-PI) copolymer systems in organic solvents and found that the enthalpy is solely responsible for micellization.^{15–19} Furthermore, they pointed out that the length of the core forming block has an appreciable effect on ΔG° and ΔH° , while the length of the soluble block does not have a clear effect on ΔG° .^{16,17} Quintana et al. studied PS-*b*-PEP copolymer systems in different organic environments and found that the composition of the solvent mixtures markedly influences the ΔG° , ΔH° , and ΔS° values and also that enthalpy is the driving force for micellization.^{20,21,25,26} Chu and co-workers studied poly(*tert*-butylstyrene)-*b*-polystyrene (P(*t*-BS)-*b*-PS) diblock and poly(*tert*-butylstyrene)-*b*-polystyrene-*b*-poly(*tert*-butylstyrene) (P(*t*-BS)-*b*-PS-*b*-P(*t*-BS)) triblock copolymers in organic solvents and reached the same conclusions.^{22,24} PEO-*b*-PPO-*b*-PEO and PPO-*b*-PEO-*b*-PPO (PEO and PPO stand for poly(ethylene oxide) and poly(propylene oxide), respectively) copolymer systems in aqueous media have also been studied by several research groups.^{19,23,27–29,31,34} For these systems, it was found that the micellization process is entropy-driven, similar to that in small molecule surfactant systems.^{35–37} Both Chu's²³ and Hatton's^{27,28} groups tried to associate molecular architecture with the thermodynamics of micelle formation, but the effects of various block lengths on the thermodynamics were not elucidated systematically.

Since we are interested in crew-cut aggregates and since no thermodynamic studies have been performed on these systems to date, a thermodynamic study appears useful. Also, to our knowledge, there have been no studies in which the effects of several relevant factors on thermodynamics of micellization have been investigated quantitatively for the same system. As was mentioned above, entropy-driven processes are associated with aqueous media, while enthalpy-driven processes are connected with organic solvents. In our system, the crew-cut micelles are formed in a mixture of an organic solvent and water. Therefore, it is of interest to know what will happen in such a medium as the ratio of the solvent components changes.

In the present paper, we report on the thermodynamics of micellization of crew-cut spherical micelles formed from PS-*b*-PAA copolymers in DMF/H₂O mixtures. In particular, we study the effects of four variables, i.e., water, insoluble block (PS) length, soluble block (PAA) length, and NaCl concentration, on the thermodynamic functions (ΔG° , ΔH° , and ΔS°). By use of the closed association model, the standard thermodynamic functions are determined and correlated with the copolymer composition, the solvent composition, and the NaCl content. Furthermore, combined equations for the thermodynamic functions for all the factors are obtained by fitting of the experimental data. The effect of homopolystyrene on the SLS behavior is also studied.

2. Experimental Section

2.1. Block Copolymers. The polystyrene-*b*-poly(*tert*-butyl acrylate) diblock copolymers were synthesized by sequential anionic polymerization of styrene followed by *tert*-butyl acrylate (*t*-BuA) using *sec*-butyllithium as the initiator.³⁸ The polymerization was carried out in tetrahydrofuran (THF) at -78°C under nitrogen. After the polystyrene block was formed, an

aliquot of the reaction mixture was withdrawn for characterization. Then a series of diblock copolymers with the same polystyrene block length were obtained by withdrawing aliquots of the mixtures after each *t*-BuA addition. The degree of polymerization and the polydispersity of the polymers were determined by gel permeation chromatography (GPC). The homopolystyrene and all the diblock copolymers in the form of *t*-BuA gave one narrow GPC peak. FTIR was used to measure the degree of polymerization of the poly(*t*-BuA) block.³⁸ The poly(*t*-BuA) blocks in the copolymers were hydrolyzed to their acid form in toluene using *p*-toluenesulfonic acid as the catalyst. A detailed description of the procedures can be found elsewhere.³⁸ The polymers are identified by the notation used previously.⁶ For example, 170-*b*-59 represents a diblock copolymer containing 170 styrene repeat units and 59 acrylic acid repeat units (number average), while 500-*b*-0 represents homopolystyrene with 500 repeat units.

2.2. Fractionation of Block Copolymers. In anionic polymerization, the copolymer frequently contains some homopolymer because chain termination may have taken place while adding the monomer for the second block. To separate the homopolystyrene from the PS-*b*-PAA copolymers, the samples were first dissolved in THF. Then sodium hydroxide (NaOH) (100% molar ratio relative to acrylic acid) in aqueous solution was added to the THF solution, which converted the acrylic acid blocks to sodium acrylate blocks. Reverse micelles of star type, with a poly(sodium acrylate) core and a polystyrene corona, were formed in the solution, and a bluish color appeared. By addition of an appropriate amount of deionized water, the reverse micelle phase separated from the solution, forming a heavier liquid phase at the bottom because of the micelles' much higher apparent molecular weights; the homopolystyrene still remained soluble in the THF/H₂O mixtures.⁹ The upper clear solution containing the homopolystyrene was withdrawn and the micelles were left at the bottom. The micelles were redissolved and the process was repeated two or three times until no homopolystyrene could be detected in the solutions by GPC. It should be recalled that these solutions now consist of micelles and single chains (i.e., homopolystyrene) and that GPC can detect micelles vs single chains, although it cannot differentiate between single copolymer chains and homopolystyrene. However, even if no single chain peak is seen, the copolymers may still contain trace amounts of homopolystyrene due to the detection limits of GPC.

To convert the sodium acrylate blocks back to the acrylic acid form, the micelles were stirred with a mixture of 15% acetic acid, 5% deionized water, and 80% THF overnight, precipitated into the mixture of 95% methanol, 4% deionized water, and 1% hydrochloric acid, and stirred overnight. This procedure was repeated several times until no reverse micelles could be detected in the THF solutions by SLS. The homopolystyrene and the diblock copolymers (before and after fractionation) used in this study are listed in Table 1.

2.3. Sample Preparation. For the SLS measurements, the stock solutions (ca. 1–3 wt %) were prepared by dissolving the block copolymer samples in *N,N*-dimethylformamide (DMF, H₂O \leq 0.05%, ANACHEMIA), which is a common solvent for both blocks, and were stored for at least 24 h in glass tubes sealed with Teflon tape. These stock solutions were filtered directly into the scintillation vials (diameter = 2.5 cm) through filters of 0.45 μm pore size and diluted with DMF solvent filtered through the same size filters. Finally, the proper amount of deionized water (filtered through filters of 0.22 μm pore size) was added. To study the NaCl salt effect, a calculated amount of NaCl in aqueous solution, filtered through 0.22 μm filters,

TABLE 1: Molecular Characteristics of Homopolystyrene and of Polystyrene-*b*-Poly(acrylic acid) Diblock Copolymers before and after Fractionation

before fractionation			after fractionation	
PS- <i>b</i> -PAA	M_w/M_n	% homo PS ^a	PS- <i>b</i> -PAA ^b	M_w/M_n ^c
500- <i>b</i> -0	1.04			
170- <i>b</i> -59	1.08	0	170- <i>b</i> -59	1.08
500- <i>b</i> -58	1.04	4.5	500- <i>b</i> -60	1.04
740- <i>b</i> -55	1.08	9.5	740- <i>b</i> -60	1.08
740- <i>b</i> -110	1.08	9.5	740- <i>b</i> -120	1.08
740- <i>b</i> -180	1.08	9.5	740- <i>b</i> -195	1.08

^a Homopolystyrene content was determined by GPC and is given in wt %. ^b PAA block lengths were recalculated after fractionation based on the amount of removed homopolystyrene. ^c The polydispersity indices, after fractionation, are considered to be the same as before because of the short PAA block lengths and small amount of homopolymer removed from the original copolymers.

was added into the scintillation vials. Then the deionized water was added until the required water content was reached. The scintillation vials were covered tightly and sealed with Teflon tape. The vials were heated to 80–90 °C for 2 h to ensure that the copolymers were in their single-chain state before the start of the SLS measurements. The filters used were always rinsed first with 20 mL of solvent prior to solvent and sample filtration in order to remove any possible contaminants. Also, the filters were rinsed with 4 mL of stock solution prior to sample collection, which would saturate any possible adsorption sites on the filters.

2.4. Light Scattering Measurements. The light scattering experiments were performed on a DAWN-F multiangle laser photometer (Wyatt Technology, Santa Barbara, CA) at 15 angles, from 26 to 137°. The instrument is equipped with a He–Ne laser (632.8 nm). The measurements were performed by decreasing the temperature and monitoring the scattered light intensity at a 90° scattering angle. For each measurement, the solutions were allowed to sit at a given temperature for 40 min to ensure that the solutions had reached equilibrium. For one of the solutions, the measurements were repeated three times by both increasing and decreasing the temperature. The results were reproducible in that the cmt difference determined from the heating or cooling runs was 0.5 °C, which is within the experimental error of the measurements.

3. Thermodynamics of Block Copolymer Micellization

It is well established that block copolymers form micelles in selective solvents. In general, micellization of block copolymers, as of small molecule surfactants, obeys the closed association model,^{1,15} which assumes an equilibrium between molecularly dispersed copolymer chains (unimers) and multi-molecular aggregates (micelles) with a constant association number (m). Thus, the standard Gibbs free energy of micellization per mole of copolymer chains transferred from the ideal dilute copolymer solution to the micelle cores is given by^{36,37}

$$\Delta G^\circ \approx RT \ln(\text{cmc}) - RTm^{-1} \ln([A_m]) \quad (1)$$

where cmc is the critical micelle concentration and $[A_m]$ is the concentration of micelles.

When the association number is high, the second term of eq 1 is very small and can be neglected. Equation 1 then becomes

$$\Delta G^\circ \approx RT \ln(\text{cmc}) \quad (2)$$

If the association number and ΔH° are independent of temperature, the following relation can be obtained from eq 2

using the Gibbs–Helmholtz equation:^{36,37}

$$\Delta H^\circ \approx R \frac{d \ln(\text{cmc})}{dT} \quad (3)$$

This equation allows one to estimate the contribution of the enthalpy term to ΔG° of the micellization. From a knowledge of both ΔG° and ΔH° , ΔS° can be determined from

$$\Delta S^\circ = (\Delta H^\circ - \Delta G^\circ)/T \quad (4)$$

For the thermodynamic study of the copolymer micellization using SLS, it is more convenient to carry out experiments in which the scattered light intensity is monitored over a range of temperatures to find the critical micelle temperature (cmt) at a constant concentration. Thus, the cmc and temperature can be replaced by concentration (C) and cmt (T_{cmt}), respectively. Equations 2–4 then become

$$\Delta G^\circ \approx R(T_{\text{cmt}}) \ln C \quad (5)$$

$$\Delta H^\circ \approx R \frac{d \ln C}{d(T_{\text{cmt}})} \quad (6)$$

$$\Delta S^\circ = (\Delta H^\circ - \Delta G^\circ)/T_{\text{cmt}} \quad (7)$$

To compare the thermodynamic functions from different studies, it is necessary to keep in mind that there is a considerable difference in the numerical value of the standard Gibbs free energy and standard entropy when different standard states are chosen.^{36,37} In the literature, the free copolymer chains and micelles in ideal dilute solutions at unit molarity or at unit mole fraction have been chosen frequently as standard states.

4. Results and Discussion

The Results and Discussion section is divided into five parts. In the first part, the method of determining the critical micelle temperature is presented and compared with methods described in the literature. The second part discusses the effects of fractionation and the addition of homopolystyrene on the measured cmcs, as well as some anomalies in the SLS studies. The estimation of standard thermodynamic functions, according to the closed association model, is given in the third part. The fourth part addresses the effects of water content, PS block length, PAA block length, and NaCl concentration on the thermodynamic functions and presents combined equations for all the factors. In the final part, we compare our results with those of other researchers in both the copolymer and small molecule surfactant fields.

4.1. cmt Determination. The micellization process is a function of temperature. The temperature at which the presence of micelles in the solution can just be detected is considered as the critical micelle temperature (cmt). Figure 1 shows the plots of the scattered light intensity at a 90° angle against temperature for the fractionated copolymer 500-*b*-60, with two different copolymer concentrations, in DMF containing 4.50 wt % water. However, the details of how to determine the cmt from a given curve differ. Price et al. suggested that the cmt is located at the point at which the scattered light intensity at a 60° angle just starts to increase.¹⁵ Quintana et al. plotted the intensities at three angles (45°, 90°, and 135°) against temperature²⁰ but otherwise used the same method as that of Price. The group of Chu determined the intensity at a 45° angle and defined the intersection of two straight lines as the cmt.²² The group of Hatton also used the intersection of two straight lines at the lower temperature inflection point as the cmt value in both UV–

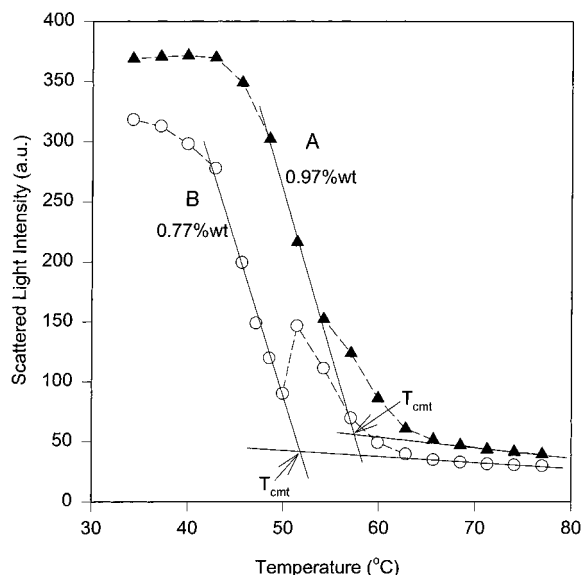


Figure 1. Plots of the scattered light intensity at a 90° angle against temperature for copolymer 500-*b*-60 in DMF containing 4.50 wt % water. Copolymer concentrations are indicated near each curve, and arrows indicate the cmcs estimated from the curves.

visible and fluorescence studies,²⁷ which is similar to Chu's method. Thus, there are basically two methods, i.e., the first upswing and the intersection of straight line segments, used to estimate cmt values.

In the present study, we tried both methods to determine the cmcs and believe that the second method is preferable in the present case. Thus, we use the intersection point of two straight lines as the cmt, as suggested by Chu et al.. For curve A in Figure 1, as the temperature decreases, a progressive increase of the scattered light intensity is seen followed by a sharp increase between ca. 60 and ca. 45 °C. After that the intensity decreases slightly. At the highest temperatures (above 65 °C), the slight increase in the scattered light intensity with decreasing temperature is probably caused by a change in coil dimensions of the free copolymer chains. In this region, only single chains are present, and the sharp increase in the scattered light intensity is a consequence of the appearance of micelles. Finally, the slight decrease of the intensity at the lowest temperatures may be due to the solidification of the micelle cores with decreasing temperature. The temperature indicated by the arrow at the intersection of the two straight lines is taken as the cmt value.

In a similar way, the cmcs were determined for the other copolymer solutions under different conditions. All the plots are similar. However, a few plots (in ca. 10% of the cases) show a so-called "anomalous" effect illustrated in curve B. For that curve, with decreasing temperature, a slow increase of the scattered light intensity is observed just as for curve A. However, here it is followed by a small peak around 50 °C and then a steep increase until ca. 40 °C. The small peak is probably associated with the precipitation of homopolystyrene (see section 4.2 for a more detailed discussion). Otherwise, the curve is similar to that shown in A. Following the suggestion of Chu et al.,²⁴ we consider that the second sharp increase is due to the appearance of micelles in the system. Thus, the cmt value, indicated by the arrow, was determined for this type of curve by the same method as used for curve A.

4.2. Effect of Homopolystyrene on the Measured cmcs and Anomalous Phenomena. Since the presence of the anomalies has been ascribed to homopolystyrene,³⁹ it is of interest to explore the effects on the scattering behavior of both the removal of the homopolystyrene (via fractionation) and the addition of various amounts of homopolymer to the diblocks.

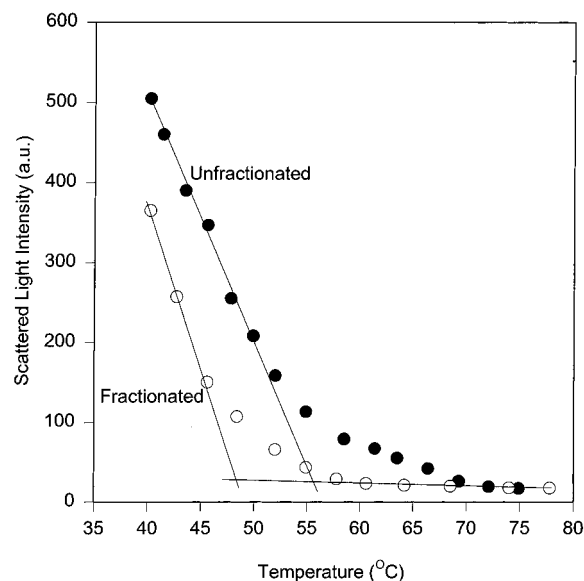


Figure 2. Plots of the scattered light intensity at a 90° angle against temperature for fractionated and unfractionated copolymer 500-*b*-58 in DMF containing 4.50 wt % water.

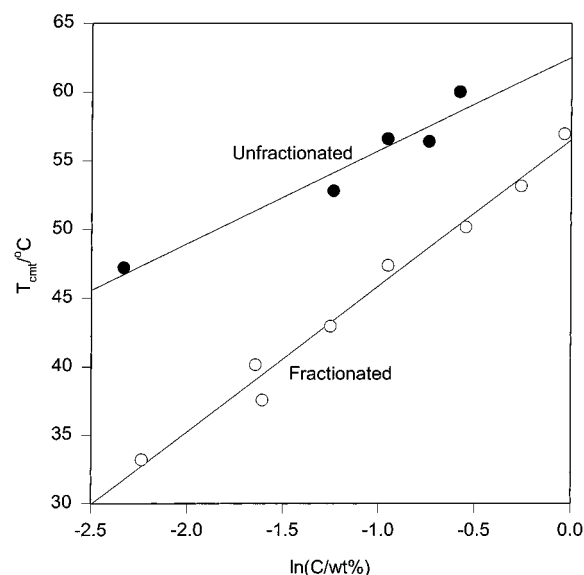


Figure 3. Plot of cmt as a function of logarithmic polymer concentration for fractionated and unfractionated copolymer 500-*b*-58 in DMF containing 4.50 wt % water.

The copolymer 500-*b*-58, which contains 4.5 wt % homopolystyrene, was used to study the fractionation effect on the cmcs. After fractionation, we recalculated the polymer composition from the amount of removed homopolystyrene. The calculated value then became 500-*b*-60 (see Table 1). The plots of the scattered intensity against temperature for 0.39 wt % polymer in DMF in the presence of 4.50 wt % H₂O are shown in Figure 2 for samples both before and after fractionation. Similar results for other polymer concentrations are given in Figure 3, which shows the plots of the cmcs (T_{cmt}) as a function of $\ln(C/\text{wt } \%)$. It is clear that fractionation has an appreciable effect on the measured cmt values. Therefore, fractionation is desirable before performing the thermodynamic studies in order to obtain more precise thermodynamic functions for the micellization process.

As a complement to the fractionation experiments, we also studied the influence of homopolystyrene content on the cmcs for the 500-*b*-60 copolymer. Figure 4A shows the plots of the scattered light intensity as a function of temperature for different

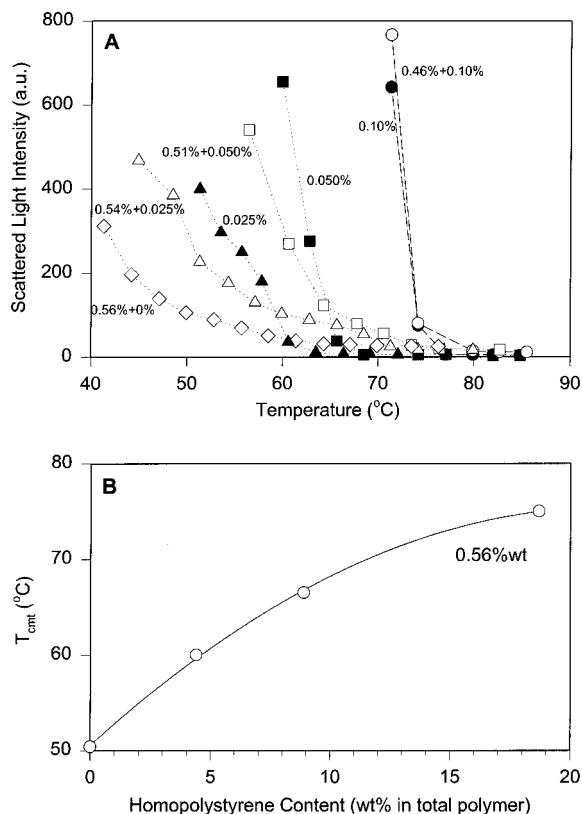


Figure 4. (A) Plots of the scattered light intensity at a 90° angle against temperature for PS (500) (closed symbols) and fractionated copolymer 500-*b*-60 containing different amounts of PS(500) (open symbols) in DMF containing 4.50 wt % water. The sample labeled *x*% contains *x* wt % homopolymer, and the sample labeled *y*% + *z*% contains *y* wt % copolymer and *z* wt % homopolymer. (B) Plot of cmt as a function of PS (500) content in the total polymer for copolymer 500-*b*-60 in DMF containing 4.50 wt % water. The total polymer concentration is indicated on the graph.

ratios of homopolystyrene 500 and copolymer 500-*b*-60 (open symbols) as well as the pure homopolystyrene (closed symbols). All these samples were studied in DMF containing 4.50 wt % water. It should be stressed that, in the experiments involving mixtures, the total polymer content was kept constant at 0.56 wt %. The sample labeling indicates the content of both components. Thus, the sample labeled 0.51% + 0.050% contains 0.51 wt % copolymer and 0.050 wt % homopolystyrene. From this plot, the measured $cmts$ were determined in the usual way (analogous to that shown in Figure 1). Figure 4B shows a plot of the measured cmt (T_{cmt}) against the homopolystyrene content in the total polymer. It is clear that as the homopolystyrene content increases, the measured $cmts$ increase.

In addition to the results for the mixtures, Figure 4A also shows the scattered light intensity as a function of temperature for the pure homopolystyrene. It is of interest to compare the curve containing 0.46 wt % copolymer and 0.10 wt % homopolymer, with the curve showing the results for the 0.10 wt % homopolymer alone. As can be seen, the location of the curves is nearly identical, indicating that it is the homopolymer that dominates the position of the micellization curve in this case. However, as the homopolymer content decreases (i.e., to 0.050 or 0.025 wt %), one sees that the distance between the homopolymer curve and the curve of the copolymer containing that amount of homopolymer increases, suggesting that as the homopolymer content decreases, the micellization process of the copolymer becomes more and more important.

Another factor that is very useful for studying these phe-

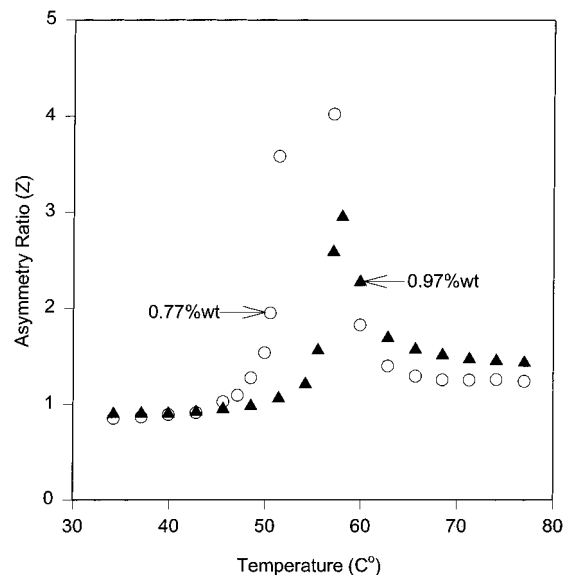


Figure 5. Plots of the asymmetry ratio against temperature for solutions of copolymer 500-*b*-60 at two concentrations in DMF containing 4.50 wt % H_2O .

nomena is the asymmetry factor *Z* representing the ratio of the scattered light intensities at 45° and 135° angles. *Z* is related to the size and the shape of the scattering particles. Optically clean solutions of small macromolecular particles should have a *Z* value near unity.⁴⁰ Several research groups have investigated the asymmetry factor *Z* as a function of temperature near the onset of the micellization and found that there is a peak that in some cases appears at the same temperature as the peak in the scattering curve (see Figure 1).^{20,39,41-43} We also observed a maximum in the plot of *Z* as a function of temperature. This is shown in Figure 5 for the 0.77 and 0.97 wt % fractionated block copolymer samples in DMF containing 4.50 wt % water. The maximum here occurs at a point just before micelle formation (see Figure 1). It should be noted that the samples for both Figures 1 and 5 are same. It is clear that for the 0.77 wt % sample, the effect is much larger than that for the 0.97 wt % sample. At both high-temperature (above 65 °C) and low-temperature regions (below 55 °C for the 0.97 wt % sample and 50 °C for the 0.77 wt % sample), the *Z* values are around 1 and give no angular asymmetry, suggesting that the particles are likely small. From the point of view of detecting the anomalies, the curve of *Z* versus *T* is even more sensitive than the plot of the scattered light intensity versus *T*.

From the phenomena discussed above, it appears that the detailed shapes of the scattering curves, and especially the positions of the measured $cmts$, are due to two contributions. One is micelle formation of the block copolymer, the other the precipitation of the homopolystyrene. The shape of the scattering curves reflects a combination of these two effects. When micelle formation is the dominant process, the plots of the scattered intensity versus temperature are normal, resembling curve A in Figure 1. In copolymers containing a relatively high homopolystyrene content, the scattered intensity change is dominated by precipitation, and the plots again look relatively normal (see unfractionated curve in Figure 2) but moved to a higher temperature. Anomalous phenomena (e.g., the peak in Figure 1) only appear in the rare event that both micellization and precipitation processes are of comparable importance. Under those circumstances, one obtains plots that are similar to curve B in Figure 1.

4.3. Estimation of Thermodynamic Functions from $\ln(C/wt \%)$ versus T_{cmt}^{-1} Plots. To minimize the influence of

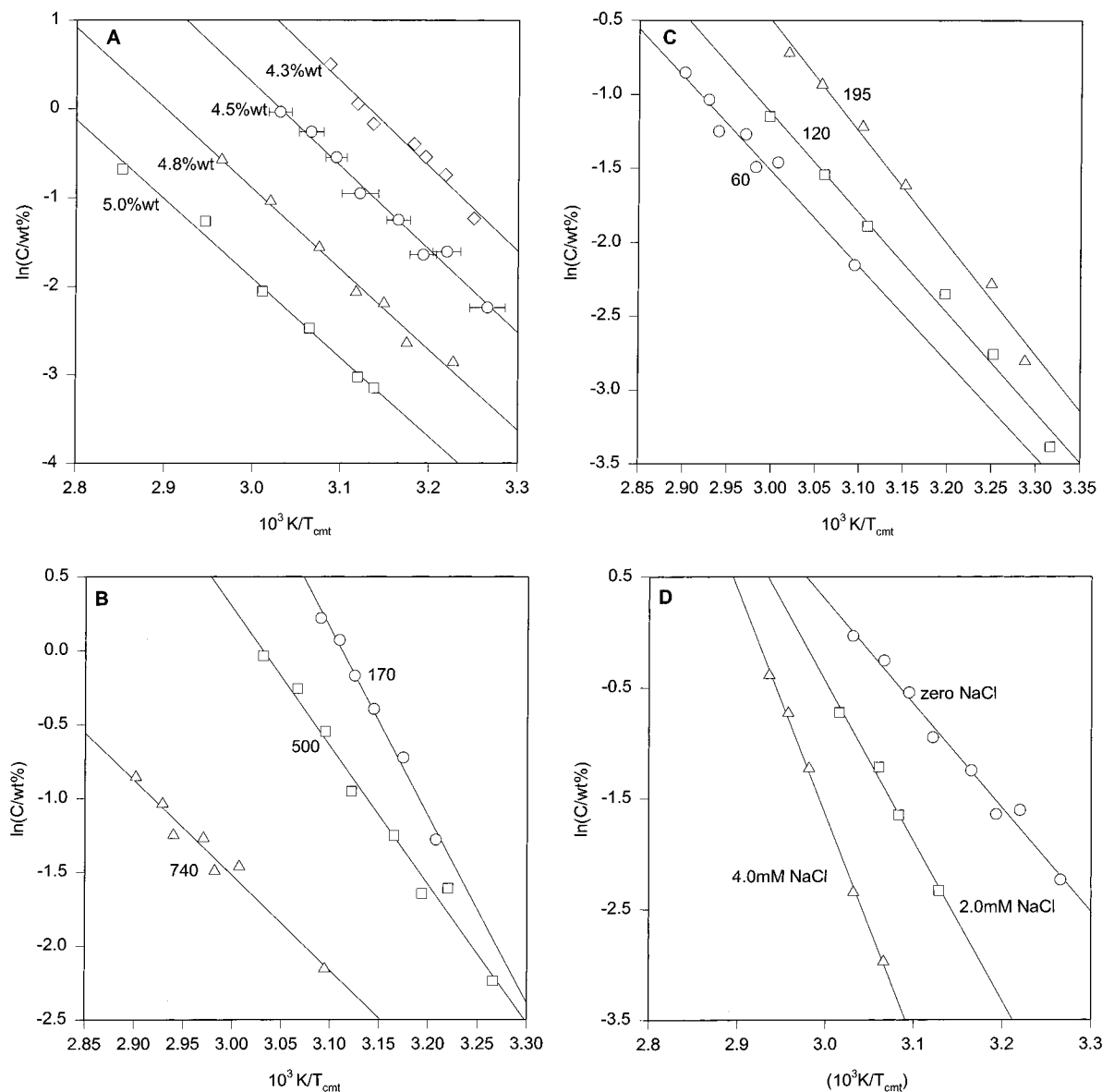


Figure 6. Logarithmic copolymer concentration as a function of the reciprocal of the cmc (K): (A) copolymer 500-*b*-60 in DMF with various water content, where, for 4.50 wt % H_2O , the error bars indicate the uncertainties estimated from the determination of cmcs; (B) copolymers with PAA blocks of 60 ± 1 units and different PS block lengths in DMF with 4.50 wt % water; (C) copolymers with the same PS block (740) and different PAA block lengths in DMF with 4.50 wt % water; (D) copolymer 500-*b*-60 in DMF with different NaCl content and a constant 4.50 wt % water content.

homopolystyrene, all the copolymers were fractionated before performing the thermodynamic study. Also, it is worth noting that the spherical micelles isolated from solutions for this system have a narrow size distribution ($\text{PI} < 1.01$) and a high association number (over 100).^{5,6} Therefore, the closed association model, or eqs 5–7, can be used to treat experimental data.

As suggested by eq 6, the logarithm of copolymer concentrations in wt % is plotted as a function of the reciprocal cmc (K^{-1}) in Figure 6. The figure contains four graphs. In each of these, different variables are changed. Graph A shows the effect of the water content in DMF for copolymer 500-*b*-60. Graph B gives the plots for block copolymers with similar PAA block lengths (approximately 60) but different PS block lengths in DMF containing 4.50 wt % water. Graph C shows the relations for copolymers with various PAA block lengths but the same PS block length (740) in DMF again for 4.50 wt % water. Graph D presents the effect of the NaCl content for copolymer 500-*b*-60 in DMF, again with 4.50 wt % water. All these plots are linear with correlation coefficients above 0.97. From these plots,

the standard enthalpies (ΔH°) were determined using eq 6. Once the standard enthalpies were obtained, the standard Gibbs free energies (ΔG°) were obtained from the cmc at 25 °C by using eq 5. Finally, the standard entropies (ΔS°) were calculated from both terms using eq 7. The values of these standard thermodynamic functions, along with the cmc values, are given in Table 2. The values listed are per mole of copolymer chains transferred from the ideal dilute solutions to the micelle cores and are calculated using the molarity as the unit of copolymer concentration. The uncertainties in ΔH° in Table 2 represent the standard deviations from the determination of ΔH° . As can be seen, all the standard thermodynamic functions of micelle formation are negative for the conditions studied. Thus, the micellization process is an exothermic process. Furthermore, it is seen that the standard entropy of micellization is unfavorable and that the standard enthalpy drives the process and is thus solely responsible for micelle formation.

The negative standard enthalpy, or exothermicity, is mainly due to the change from the unfavorable interactions between the polystyrene segments and solvent to the more favorable

TABLE 2: Thermodynamic Data of "Crew-Cut" Micellization of PS-*b*-PAA Copolymers in DMF/H₂O Mixtures under Different Conditions

copolymer PS- <i>b</i> -PAA	H ₂ O (wt%)	NaCl (10 ⁻³ mol L ⁻¹)	cmc _{298K} (mol L ⁻¹)	ΔH° ^a (kJ mol ⁻¹)	ΔG° _{298K} (kJ mol ⁻¹)	ΔS° (J mol ⁻¹ K ⁻¹)
500- <i>b</i> -60	4.30	0.0	1.96 × 10 ⁻⁵	-79.5 ± 6.2	-26.9	-177
	4.50		8.13 × 10 ⁻⁶	-77.8 ± 4.3	-29.0	-164
	4.80		2.67 × 10 ⁻⁶	-75.6 ± 3.7	-31.8	-147
	5.00		1.04 × 10 ⁻⁶	-74.3 ± 3.3	-34.1	-135
	4.50	2.0	6.43 × 10 ⁻⁷	-119.7 ± 5.2	-35.3	-283
170- <i>b</i> -59			2.28 × 10 ⁻⁸	-169.3 ± 5.0	-43.6	-422
			1.92 × 10 ⁻⁵	-105.4 ± 4.2	-26.9	-263
740- <i>b</i> -60		0.0	2.58 × 10 ⁻⁶	-53.5 ± 5.1	-31.9	-72.7
740- <i>b</i> -120			3.20 × 10 ⁻⁶	-56.1 ± 2.7	-31.4	-83.1
740- <i>b</i> -195			4.30 × 10 ⁻⁶	-62.8 ± 3.5	-30.6	-107

^a The uncertainties in ΔH° represent the standard deviations from the average of two-point calculations.

interactions of polystyrene/polystyrene and solvent/solvent accompanying the micellization process.^{1,44} Other contributions may include interactions involving the corona-forming block,⁴⁴ hydrogen bond formation in the solvent,⁴⁵ and the interface energy between the micelle core and solvent. The negative standard entropy, in the present situation, is mainly due to the decrease of the number of particles after micelle formation, which can be explained using simple statistics.^{1,15} Other contributions to the entropy may involve conformational changes of the two blocks⁴⁴ and the change of the solvent structure.⁴⁵ These contributions to the enthalpy and entropy will be discussed in section 4.4.

4.4. Factors Affecting the Standard Thermodynamic Functions. This part of the paper discusses the effects of various factors, i.e., solvent composition, insoluble and soluble block lengths, and NaCl content on the standard thermodynamic functions. The effect of each of these factors is expressed by equations for ΔG°_{298K}, ΔH°, and ΔS°. In addition, combined equations, which take into account all of the factors, are given at the end of this part.

4.4.1. Water Content. The variations of the standard Gibbs free energy at 25 °C, the standard enthalpy, and the standard entropy of micellization as a function of water content in DMF are plotted in Figure 7A for copolymer 500-*b*-60. From the plots, the following equations are obtained:

$$\Delta G^{\circ}_{298K} = (17.0 - 10.2W_{H_2O})/(\text{kJ mol}^{-1}) \quad (r^2 = 0.998) \quad (8)$$

$$\Delta H^{\circ} = (-111 + 7.38W_{H_2O})/(\text{kJ mol}^{-1}) \quad (r^2 = 0.997) \quad (9)$$

$$\Delta S^{\circ} = (-430 + 59.0W_{H_2O})/(\text{J K}^{-1} \text{ mol}^{-1}) \quad (r^2 = 0.999) \quad (10)$$

where W_{H_2O} is the water content in wt % and r^2 is the correlation coefficient. At 25 °C, ΔG° decreases linearly with water content. This suggests that the higher the water content, the lower the ΔG° and therefore the lower the cmc. This reflects the fact that as water is added, the quality of solvent worsens for the PS block. It will be shown later that, as might be expected, the quality of solvent simultaneously improves for the PAA block. The overall effect is to make micellization easier. Although we only studied a very narrow range of water content (4.3–5.0 wt %), it may be of interest to extrapolate the water content over a wider range to see the influence of that variable, at least qualitatively. If we extrapolate to lower water content, it is found that the water content must be above ca. 2 wt % to obtain a negative ΔG°. Below that water content, it is impossible to form micelles, as has been found experimentally in a previous study.⁹ If the water content is extrapolated to 15

wt %, the cmc value at 25 °C is ca. 1×10^{-24} M, suggesting that there is less than one free copolymer molecule per liter of solution. Of course, this number should not be interpreted quantitatively, but it does show that the cmc is very low at room temperature.

In small molecule surfactant systems, micellization is accompanied by an appreciable change in the water structure (the "hydrophobic effect").⁴⁵ This change has a pronounced effect on the thermodynamic functions, notably the entropy of micellization. In the present system, owing to the presence of water (4.3–5.0 wt % \approx 15–20 mol %) in the solvent mixture, the hydrophobic effect probably also contributes to the thermodynamic functions. From the standard enthalpy, before micelle formation, the water molecules, which surround the insoluble PS blocks, form a very strong hydrogen-bonded network. Upon micellization, as a result of the transfer of the PS blocks into the hydrophobic micelle cores, the strong hydrogen-bonded network is destroyed and the more normal water structure with a weaker network of hydrogen bonds is probably regenerated. This regeneration of the normal water structure is an endothermic process. Therefore, the standard enthalpy increases with increasing water content. The fact that only a small change of enthalpy is visible on the graph is due to the fact that the change of the water content in the plot is very small. If the water content is extrapolated to a higher level, e.g., 15 wt %, ΔH° becomes positive and is no longer a driving force for micelle formation. This, however, may not be accessible experimentally because of the extremely low cmc at that point.

It can also be seen from eq 10 and Figure 7A that ΔS° increases linearly with increasing water content. This increase of ΔS° may be due to the hydrophobic effect. Before micellization, the water forms a highly hydrogen-bonded shell around the hydrophobic chains.⁴⁵ This shell is broken down upon micellization. This may contribute significantly to the increase of the entropy. The higher the water content, the greater the contributions of the hydrophobic interactions between PS block and water molecules, and the more ordered the water structure formed before micelle formation. Upon micellization, the more normal water structure is regenerated. Thus, the standard entropy increases with increasing water content. Not surprisingly, at low water content, ΔS° is highly negative and comparable to the negative entropy of micellization of both small molecule surfactants and copolymers in organic solvents. At higher water content (above 7.5 wt %), ΔS° may become positive, resembling the situation in aqueous media. This indicates that above that concentration, ΔS° may drive micelle formation by making a negative contribution to the standard free energy.

From the above qualitative discussion, it appears that at low water content (<7.5 wt %), micelle formation is an exothermic

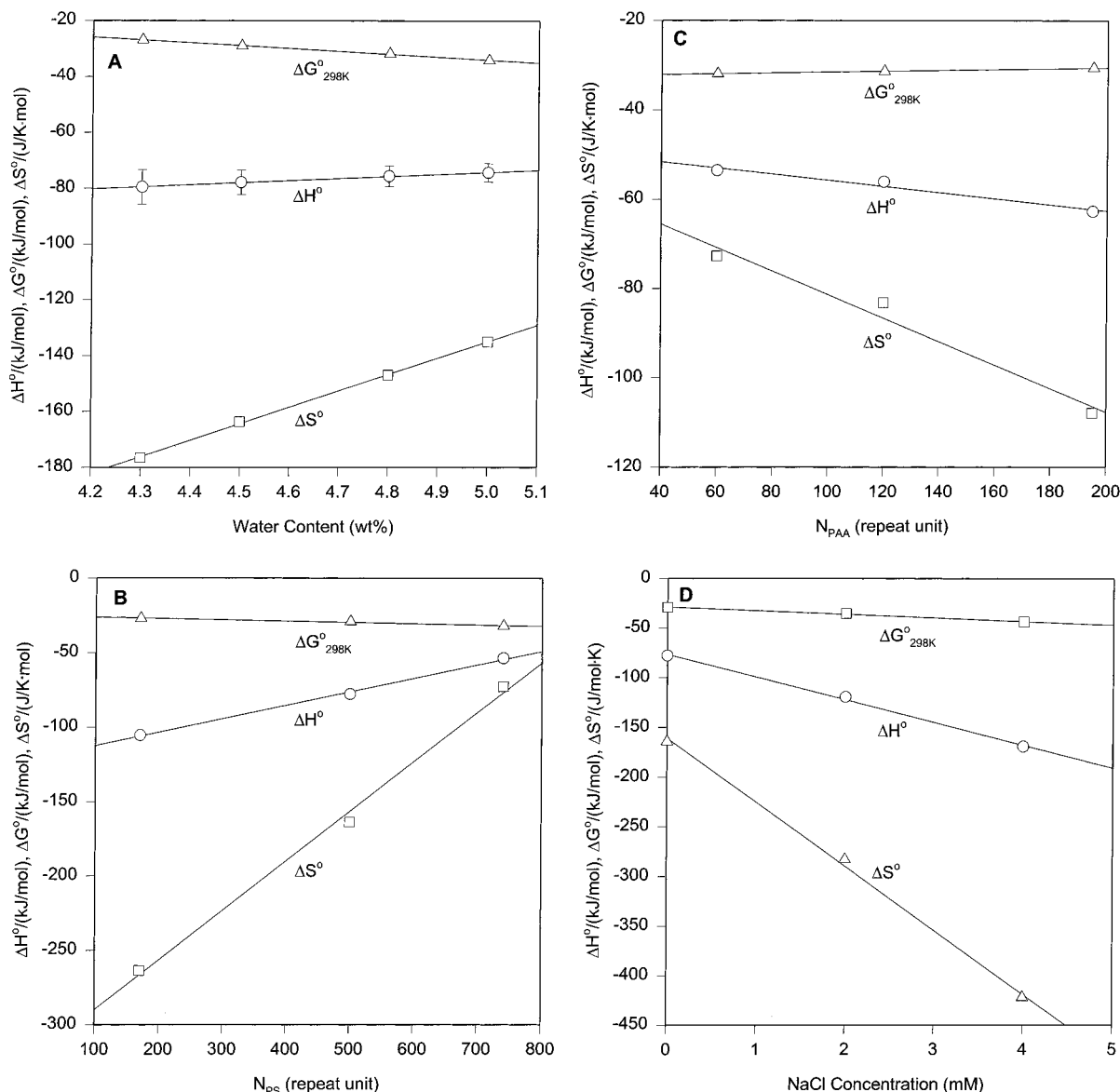


Figure 7. Effects of different variables on thermodynamic functions for micellization in DMF/H₂O mixtures: (A) water content (for copolymer 500-*b*-60), where the error bars are the standard deviations in ΔH° ; (B) PS block length (for copolymers with PAA blocks of 60 ± 1 units in DMF containing 4.50 wt % water); (C) PAA block length (for copolymers with the same PS block 740 in DMF containing 4.50 wt % water); (D) NaCl concentration (for copolymer 500-*b*-60 in DMF containing 4.50 wt % water).

process and the standard enthalpy is solely responsible for micellization, in parallel with the micellization behavior of other systems in organic solvents. As the water content increases (from 7.5 to 15 wt %), the standard entropy may turn positive and drive micelle formation along with the standard enthalpy. At still higher water content (> 15 wt %), the micelle formation may become an endothermic process and the standard entropy is possibly the only driving force, again in parallel with the micellization behavior of other systems in aqueous media. Since the standard Gibbs free energy is a combination of two contributions, it decreases with increasing water content due to the predominance of $T\Delta S^\circ$ component.

4.4.2. Insoluble (PS) Block Length. The effect of the PS block length on the thermodynamic functions is shown in Figure 7B. The diblocks used in this study are copolymers with approximately 60 units of PAA and various PS block lengths, and the solvent is DMF containing 4.50 wt % water. It is clear that the effect of the PS block is similar to that of the water content because for both cases, the environment becomes poorer for the core forming block with an increase of both variables. From the curves, linear equations for all thermodynamic

functions are obtained and are given in eqs 11–13,

$$\Delta G^\circ_{298K} = (-25.2 - 0.00859N_{PS})/(\text{kJ mol}^{-1}) \quad (r^2 = 0.980) \quad (11)$$

$$\Delta H^\circ = (-122 + 0.0906N_{PS})/(\text{kJ mol}^{-1}) \quad (r^2 = 0.997) \quad (12)$$

$$\Delta S^\circ = (-323 + 0.333N_{PS})/(\text{J K}^{-1} \text{mol}^{-1}) \quad (r^2 = 0.996) \quad (13)$$

where N_{PS} is the number of styrene units in the PS block. It is of interest to note that even for a zero PS block length, the ΔG° of micellization is still negative. Since at that point the polymer can be stable in the solution as PAA single chains, the reason for the negative value is not clear.

To understand the Gibbs free energy well, it is useful to consider its two components (i.e., ΔH° and ΔS°). The effect of the PS block on the standard enthalpy appears very straightforward. The longer the PS block, on a molar basis, the more hydrophobic groups there are and the greater the effect

on the water molecules at a constant water content. Therefore, the longer the PS block, the more important the hydrophobic interactions and the greater the change of the water structure on micellization in terms of destruction of the strongly hydrogen-bonded water shell around PS block. Since the destruction of the shell is endothermic, the higher the PS block length, the less the negative standard enthalpy. In addition, the interface energy between the micelle core and solvent may also contribute. Since the specific area per polymer chain exposed on the micelle core surface increases with increasing PS block length, more unfavorable interactions between the PS segments and the solvent molecules remain during micellization.⁶ It is of interest to note that when the PS block length reaches 1400, ΔH° may become positive and ΔS° becomes the driving force. Unlike the situation with water content (see section 4.4.1), the driving force may change at a cmc of ca. 3×10^{-7} M, a point that is experimentally accessible.

As can be seen in eq 13, the standard entropy also increases as the PS block length increases. Since the aggregation number increases with increasing PS block length,⁵ it might at first appear that the entropy should decrease. Obviously, the opposite is the case. Therefore, the hydrophobic effect is probably again involved, in parallel with the previous suggestion. Thus, at a constant water content, the longer the PS block, the greater the destruction of the water structures after micelle formation, and then the less negative the standard entropy change. This aspect overcomes the decrease of the standard entropy due to the change in the aggregation number. Overall, the standard entropy increases. From eq 13, ΔS° does not become positive until the PS block length is above 1000 units, which indicates that after this point, the standard entropy is favorable for micelle formation and drives the micellization process, along with the standard enthalpy.

For the system at a constant water content (i.e., 4.5 wt % H₂O) and a constant PAA soluble block length (i.e., PAA = 60 units), the enthalpy drives the micelle formation at short PS block lengths (<1000 units), similar to the influence of the water content. Both ΔH° and ΔS° drive micelle formation in the intermediate PS block length region (i.e., between 1000 and 1400 units), and for PS block lengths greater than 1400 units, ΔS° is solely responsible for micellization.

4.4.3. Soluble (PAA) Block Length. The effect of the PAA block length on the thermodynamic functions is shown in Figure 7C. The diblocks in this study are the copolymers with 740 units of PS but different PAA block lengths, and the solvent is DMF containing 4.50 wt % water. Not surprisingly, the effect of the PAA block on micellization is opposite to that of the PS block. The effect on the thermodynamic functions is summarized in eqs 14–16,

$$\Delta G^\circ_{298K} = (-32.4 + 0.00938N_{PAA})/(\text{kJ mol}^{-1}) \quad (r^2 = 0.999) \quad (14)$$

$$\Delta H^\circ = (-48.8 - 0.0692N_{PAA})/(\text{kJ mol}^{-1}) \quad (r^2 = 0.976) \quad (15)$$

$$\Delta S^\circ = (-55.0 - 0.264N_{PAA})/(\text{J K}^{-1} \text{ mol}^{-1}) \quad (r^2 = 0.973) \quad (16)$$

where N_{PAA} is the number of acrylic acid repeat units in the PAA block. ΔG° increases with increasing PAA block length. Correspondingly, the cmc increases, and micelle formation becomes more difficult. Thus, the solubility of the copolymers improves as the PAA block length increases, and one can

anticipate that for extremely long PAA blocks, the diblocks may even become soluble. From a linear extrapolation, this would be expected to occur for PAA blocks of over 3500 units, suggesting that the range of micelle stability for copolymers with 740 PS units is quite large. If the effect of PAA block length is extrapolated in the opposite direction, i.e., to zero PAA block length, the standard Gibbs free energy is about $-32.4 \text{ kJ mol}^{-1}$. This negative value is consistent with precipitation of homopolystyrene in that solvent.

Considering the effect of PAA block length on the standard enthalpy, it appears that the interactions involving the corona forming block may be responsible for the change of the standard enthalpy. These probably include PAA/PAA, PAA/solvent, and solvent/solvent interactions. One can speculate that as micellization occurs for copolymers with increasing PAA block length, progressively more of the relatively less favorable PAA/solvent interactions are replaced by relatively more favorable solvent/solvent and PAA/PAA interactions. Consequently, this substitution makes a negative contribution to the standard enthalpy. It should be stressed that this explanation is speculative. In the present situation, the standard enthalpy is the sole driving force for micelle formation of the copolymers with a PS (740) block length.

As can be seen in Figure 7C and eq 16, the entropy becomes more negative with increasing PAA block length. Since, as has been shown before, the aggregation number decreases with increasing PAA block length,⁵ one would expect that the entropy should increase. Therefore, again, other effects must be involved. It is suggested that with increasing PAA block length, the PAA chains become more extended for steric reasons, and therefore, the conformational entropy decreases. This is believed to be an important component of the behavior of entropy as a function of PAA block length and appears to overcome the increase in ΔS° due to the decrease of the aggregation number. Overall, the standard entropy decreases.

4.4.4. NaCl Content. The effect of NaCl content on the thermodynamics for the copolymer 500-*b*-60 in DMF containing 4.50 wt % water is shown in Figure 7D. From the plots, the following linear relationships are obtained:

$$\Delta G^\circ_{298K} = (-28.7 - 3.65\text{mM}_{\text{NaCl}})/(\text{kJ mol}^{-1}) \quad (r^2 = 0.994) \quad (17)$$

$$\Delta H^\circ = (-76.5 - 22.9\text{mM}_{\text{NaCl}})/(\text{kJ mol}^{-1}) \quad (r^2 = 0.998) \quad (18)$$

$$\Delta S^\circ = (-161 - 64.5\text{mM}_{\text{NaCl}})/(\text{J K}^{-1} \text{ mol}^{-1}) \quad (r^2 = 0.998) \quad (19)$$

where mM_{NaCl} is the millimolar concentration of NaCl in the solution. Clearly, the effect on the thermodynamic functions is quite strong, considering that the concentration is given in millimoles per liter. The standard Gibbs free energy decreases as the NaCl content increases. This effect is opposite to that of increasing PAA block length, which confirms our previous finding in regard to the morphology study,⁸ i.e., that the effect of salt is equivalent to shortening the PAA block length. Furthermore, with added salt, the cmc decreases and micellization becomes easier.

Although the effect of increasing the NaCl content on the standard enthalpy and the standard entropy is similar to that of increasing the PAA block length, the reasons are different. It has been shown in the previous publication that with increasing salt content, the size of micelles increases, and therefore also

the aggregation number.⁸ Since the aggregation number increases, the combinatorial entropy must decrease, which appears to be the prime reason for the dramatic decrease of the standard entropy. The reason for the effect of added salt on the standard enthalpy also appears clear. The PAA chains are weakly ionized; with increasing salt content, the weak electrostatic repulsive forces between the PAA blocks decrease even further because of shielding, which makes micellization more favorable. Therefore, the standard enthalpy decreases with increasing salt content. Unlike the effect of increasing PAA block length, the decrease of the ΔH° is faster here than that of the $T\Delta S^\circ$ term. Thus, the Gibbs free energy becomes more negative.

4.4.5. Combined Equations. It is possible to combine the effects of all four variables into a single set of equations, which is given below:

$$\Delta G^\circ_{298K} = (20.4 - 0.00859N_{PS} + 0.00938N_{PAA} - 10.2W_{H_2O} - 3.65mM_{NaCl})/(\text{kJ mol}^{-1}) \quad (20)$$

$$\Delta H^\circ = (-151 + 0.0906N_{PS} - 0.0692N_{PAA} + 7.38W_{H_2O} - 22.9mM_{NaCl})/(\text{kJ mol}^{-1}) \quad (21)$$

$$\Delta S^\circ = (-574 + 0.333N_{PS} - 0.264N_{PAA} + 59.0W_{H_2O} - 64.5mM_{NaCl})/(\text{J K}^{-1} \text{mol}^{-1}) \quad (22)$$

These combined equations allow us to compare the effects of the various contributions to the total thermodynamic functions and, furthermore, to evaluate the contributions of each component to the cmc at a given temperature. Most surprisingly, it appears that the effect of changing the PAA block is almost exactly opposite to the effect of changing the PS block on the total Gibbs free energy. It is also worth noting that, in terms of the Gibbs free energy, only the PAA block makes a positive contribution, while all the other variables make negative contributions and thus favor micellization.

To evaluate the quality of the fit of these combined equations, we compare the experimental results with the values calculated using these equations. The average relative difference is 1.6%, 2.0%, and 4.7% for ΔG° , ΔH° , and ΔS° , respectively. Therefore, it appears that the equations are in good agreement with the experimental results and can be used to calculate the thermodynamics for this system. It should be kept in mind that the linearity of these equations may not be valid much beyond the range investigated. However, the trends in the thermodynamic functions are probably valid for a very much wider range.

4.5. Comparison of the Present Experimental Results with Those from Other Systems. **4.5.1. Other Block Copolymer Systems.** All the previously published studies of the thermodynamics of copolymer micellization dealt with star-like micelles.^{15–34} By contrast, we investigate a crew-cut system, which shows some differences from those for star-like systems. In the following part, we compare our results with those of the most relevant published studies.

Price et al. investigated the effect of block copolymer composition on the thermodynamics by studying the micellization of PS-*b*-PI in *n*-hexadecane.¹⁷ They compared sample PS₆₅-*b*-PI₂₅₀ ($\Delta G^\circ = -21.4 \text{ kJ mol}^{-1}$ and $\Delta H^\circ = -40.7 \text{ kJ mol}^{-1}$)⁴⁶ with sample PS₁₂₅-*b*-PI₁₉₅ ($\Delta G^\circ = -31.8 \text{ kJ mol}^{-1}$ and $\Delta H^\circ = -86.4 \text{ kJ mol}^{-1}$). These two samples have somewhat similar molecular weights for the PI blocks. They concluded that the enthalpy and free energy are strongly dependent on the molecular weight of the insoluble (PS) block. Comparing the sample PS₁₂₅-*b*-PI₁₉₅ with sample PS₁₂₀-*b*-PI₅₉₅

($\Delta G^\circ = -30.5 \text{ kJ mol}^{-1}$ and $\Delta H^\circ = -115.3 \text{ kJ mol}^{-1}$), which have PS blocks with similar molecular weights, they suggested that the effect of the soluble (PI) block on the free energy is negligible. In the present study, for copolymers with similar PAA blocks (60 ± 1 units) and PS block lengths varying from 170 to 740 units, ΔG° decreases from -26.9 to $-31.9 \text{ kJ mol}^{-1}$ while ΔH° increases from -105.4 to $-53.5 \text{ kJ mol}^{-1}$ (see Table 2). Thus, it is clear that both the free energy and enthalpy are dependent on the insoluble block length, which is in agreement with previous results.¹⁷ On the other hand, for copolymers with an identical PS block (740 units) and varying PAA blocks (in a range 60–195 units), ΔG° increases from -31.9 to $-30.6 \text{ kJ mol}^{-1}$ and ΔH° decreases from -72.7 to -107 kJ mol^{-1} (also see Table 2). The ΔG° results are, numerically, quite similar to those of Price et al.¹⁷ It is worth noting, however, that the absolute value of ΔG° per PAA repeat unit is 9.4 J and is thus even greater than that per PS repeat unit (8.6 J). Therefore, we must conclude that the free energy in this crew-cut system is dependent on both the soluble and insoluble blocks, which differs from previous experimental results on star type systems.^{17,18} The reasons behind this difference are probably related to the inherent differences between star and crew-cut systems, i.e., the short corona length.

Quintana et al. investigated the effect of the solvent composition on the thermodynamics of micellization of PS-*b*-PEP in mixtures of *n*-dodecane and 1,4-dioxane.²¹ They found that all the thermodynamic functions become less negative with increasing *n*-dodecane content in the range 10–40% but turn more negative in the range 70–100%. These results are due to the fact that micelle cores invert with changing solvent composition. Finally, they suggested that the mixture containing a selective solvent for the core-forming block may hinder the formation of micelles. This is also true in the present study. As the water content decreases, the free energy increases linearly. Simultaneously, both the enthalpy and entropy decrease linearly. Although the linearity may not continue to high water content, it is very likely that these trends are monotonic because the micelle cores cannot invert here. From the linear changes of the enthalpy and entropy, one may expect that the enthalpy and entropy would turn positive with increasing water content. Therefore, it appears that there is a transition in the driving force from enthalpy to enthalpy along with entropy, and eventually to entropy alone for micelle formation.

The effect of additives on micellization is another aspect of interest. The group of Hatton²⁹ studied the effect of urea on the thermodynamics of micellization of PEO-*b*-PPO-*b*-PEO in aqueous media; urea is generally considered to be a water structure breaker. It was found that as the urea concentration increases from zero to 4 M, ΔH° and ΔS° decrease from 330 and 1.21 to 230 kJ mol^{-1} and 0.85 $\text{kJ mol}^{-1} \text{K}^{-1}$, respectively, and ΔG°_{298K} increases from -30.6 to $-23.3 \text{ kJ mol}^{-1}$.⁴⁷ In the present study, the effect of NaCl salt on the thermodynamic functions is linear and dramatic (see Table 2). For example, with increasing NaCl concentration from zero to 4.0 mM, ΔG°_{298K} , ΔH° , and ΔS° decrease from -29.0 , -77.8 , and -164 to $-43.6 \text{ kJ mol}^{-1}$, $-169.3 \text{ kJ mol}^{-1}$, and $-422 \text{ J mol}^{-1} \text{K}^{-1}$, respectively. It is clear that this effect is far greater than that of urea in the PEO-*b*-PPO-*b*-PEO/water system. This is probably due to the fact that NaCl also changes electrostatic interactions. In addition, the added NaCl favors micelle formation, unlike urea.

4.5.2. Small Molecule Surfactant Systems. The thermodynamics of micelle formation for small molecule surfactants have been studied extensively and are relatively well understood.^{35–37,48}

Here, we only discuss those aspects that are relevant to the present study.

Considering the effect of hydrophobic chain length on the thermodynamics of micellization, for small molecule surfactants with a single straight hydrocarbon chain, the cmc is related to the number of carbon atoms in the chain (m_c) by

$$\log(\text{cmc}) = b_0 - b_1 m_c \quad (23)$$

where b_0 and b_1 are generally positive constants.³⁷ This equation can be used to describe both ionic and nonionic surfactants. The free energy of micellization thus shows a linear relationship to the number of hydrophobic units. Because b_1 is generally between 0.1 and 1, the free energy decreases at a rate of 0.24–2.4 kJ mol⁻¹ per additional carbon in the hydrocarbon chain.³⁷ In the present system, from eq 11, one can see that the relationship between the free energy and the number of hydrophobic repeat units in the PS block is similar to that of surfactants, but the free energy only decreases at a rate of 8.6 J mol⁻¹ per additional PS unit, which is far below that for surfactant systems. It should be borne in mind, however, that the small molecule systems have been studied in water, while the solvent in our system contains ca. 95 wt % of DMF.

Callaghan et al. studied the effect of 1,2-ethanediol (EG) on the thermodynamics of micellization of hexadecylpyridinium bromide in aqueous media.⁴⁸ It is worth noting that EG acts as a water structure breaker. It was found that ΔG° , ΔH° , and ΔS° change from -19.7, -46.5, and -90 at 100% EG to -48.4 kJ, -12.9 kJ, and 119 J K⁻¹ at 0% EG, respectively.⁴⁸ In that study, micelle cores are not reversible, and then the thermodynamic properties are changing monotonically. Also, at EG content above 80%, the enthalpy drives micelle formation alone, in parallel to reverse micelle systems. At EG content below 70%, both enthalpy and entropy are driving the micellization. In the present study, the micellization occurs in a DMF-rich environment, and DMF is also a water structure breaker. From eqs 8–10, it is clear that the results show trends similar to those found by Callaghan et al. The effects, however, are linear.

For small molecule surfactant systems, the effect of added salts has also been investigated extensively. The effect can be summarized by the following equations:

$$\log(\text{cmc}) = b_2 + b_3 C \quad (\text{for nonionic surfactants}) \quad (24)$$

$$\log(\text{cmc}) = b_4 + b_5 \log C \quad (\text{for ionic surfactants}) \quad (25)$$

where C is the molar salt concentration and constants b_i depend on the nature of the electrolyte.³⁷ From these two equations, it is clear that for nonionic surfactants the free energy shows a linear relationship with salt concentration, while for ionic surfactants the free energy shows a linear relationship with the log of the salt concentration. As can be seen in our study, eq 17 shows that the free energy is linearly dependent on the salt concentration, which is similar to that in nonionic surfactants. This similarity may be due to the fact that the PAA block is only weakly ionized. Therefore, the thermodynamic properties of the present system are close to those of nonionic surfactant systems. Considering that the concentrations are millimolar in the present study, NaCl shows a much more pronounced effect on the present system.

5. Conclusion

The thermodynamics of the crew-cut micelle formation of polystyrene-*b*-poly(acrylic acid) copolymer in DMF/water mixtures have been studied. All the thermodynamic functions are negative in the range investigated. Since the standard entropy

is unfavorable, the standard enthalpy is solely responsible for the micellization process. The effects of water content, NaCl content, and the PS and PAA block lengths on the thermodynamic functions were investigated systematically, and a single set of combined equations was obtained for all variables. These combined equations can be used to compare the effects of the different variables and to calculate the thermodynamic functions for this system.

The insoluble block shows a substantial effect on all the thermodynamic functions, as was observed for star type systems^{17,18} and also as predicted in a theoretical study.⁴⁴ The soluble block, however, also shows a notable effect that is almost exactly opposite to that of the insoluble block on all the thermodynamic functions. This has not been found for star-like systems.

To form micelles, the critical water concentration has to be above 2 wt % under all circumstances, which is in agreement with results of our previous study.⁹ All the thermodynamic functions vary significantly with water content. Thus, it appears that for a given copolymer, as the water content increases, the driving force for micelle formation may change from enthalpy alone to enthalpy along with entropy, and eventually to entropy only. For different copolymer compositions, the water content at the point at which the change in the driving force occurs may vary. This driving force transition involving changes in both ΔH° and ΔS° is believed to be an important phenomenon for the thermodynamics of copolymer micellization.

The added salt (NaCl) was found to influence the thermodynamic functions dramatically. The cmc decreases significantly for very small amounts of NaCl, which makes micelle formation more favorable.

No single explanation can account for all the changes in the thermodynamic properties observed here. For a salt (NaCl) free system, three situations can be differentiated. At low water content, the replacement of unfavorable PS/solvent interactions by favorable PS/PS and solvent/solvent interactions appears to be a predominant contributor to the enthalpy, while the number of the particles in the system dominates the entropy. Thus, the enthalpy is the driving force, similar to micelle formation in organic solvents. At high water content, the hydrogen-bonded network seems to dominate the micellization process. Then the entropy becomes the driving force, in parallel with micellization in aqueous media. Between high and low water content, as a result of both the above contributions, both the enthalpy and the entropy are favorable for micelle formation. For a system containing salt (NaCl), in addition to the reasons discussed for the salt-free system at low water content, electrostatic interactions in the corona region may also contribute to the enthalpy significantly. Therefore, the enthalpy is a strong driving force, while the entropy is strongly unfavorable.

Anomalies during the SLS study were also investigated. It appears that there are mainly two contributions that are responsible for the light scattering behavior. One is micellization of the block copolymer, while the other is precipitation of homopolymer. When one of the contributions is predominant, the scattered light shows normal behavior. Anomalous phenomena appear when both contribute substantially.

Acknowledgment. We gratefully acknowledge the funding of this work by the National Sciences and Engineering Research Council of Canada (NSERC).

References and Notes

- (1) Tuzar, Z.; Kratochvil, P. *Adv. Colloid Interface Sci.* **1976**, *6*, 201.
- (2) Tuzar, Z.; Kratochvil, P. In *Surface and Colloid Science*; Matijevic, E., Ed.; Plenum Press: New York, 1993; Vol. 15, p 1.

- (2) Price, C. In *Developments in block copolymers*; Goodman, I., Ed.; Applied Science Publishers: London, 1982; Vol. 1, p 39. Selb, J.; Gallot, Y. In *Developments in block copolymers*; Goodman, I., Ed.; Applied Science Publishers: London, 1985; Vol. 2, p 27. Riess, G.; Hurtrez, G.; Bahadur, P. *Encyclopedia of Polymer Science and Engineering*, 2nd ed.; Wiley: New York, 1985; Vol. 2, p 324.
- (3) Qin, A.; Tian, M.; Ramireddy, C.; Webber, S. E.; Munk, P. *Macromolecules* **1994**, 27, 120. Antonietti, M.; Heinz, S.; Schmidt, M.; Rosenauer, C. *Macromolecules* **1994**, 27, 3276. Esselink, F. J.; Semenov, A. N.; Brinke, G. ten; Hadziioannou, G.; Oostergetel, G. T. *Macromolecules* **1995**, 28, 3479. Spatz, J. P.; Mössmer, S.; Möller, M. *Angew. Chem., Int. Ed. Engl.* **1996**, 35, 1510. Shusharina, N. P.; Nyrkova, I. A.; Khokhlov, A. R. *Macromolecules* **1996**, 29, 3167.
- (4) Gao, Z.; Varshney, S. K.; Wong, S.; Eisenberg, A. *Macromolecules* **1994**, 27, 7923. Honda, C.; Sakaki, K.; Nose, T. *Polymer* **1994**, 35, 5309.
- (5) Zhang, L.; Barlow, R. J.; Eisenberg, A. *Macromolecules* **1995**, 28, 6055.
- (6) Zhang, L.; Eisenberg, A. *Science* **1995**, 268, 1728. Zhang, L.; Eisenberg, A. *J. Am. Chem. Soc.* **1996**, 118, 3168.
- (7) Zhang, L.; Yu, K.; Eisenberg, A. *Science* **1996**, 272, 1777.
- (8) Zhang, L.; Eisenberg, A. *Macromolecules* **1996**, 29, 8805.
- (9) Zhang, L.; Shen, H.; Eisenberg, A. *Macromolecules* **1997**, 30, 1001.
- (10) Guo, A.; Liu, G.; Tao, J. *Macromolecules* **1996**, 29, 2487. Ding, J.; Liu, G. *Macromolecules* **1997**, 30, 655.
- (11) Yu, K.; Eisenberg, A. *Macromolecules* **1996**, 29, 6359. Yu, K.; Zhang, L.; Eisenberg, A. *Langmuir* **1996**, 12, 5980.
- (12) Yu, Y.; Zhang, L.; Eisenberg, A. *Langmuir* **1997**, 13, 2578. Yu, Y.; Eisenberg, A. Manuscript in preparation.
- (13) de Gennes, P. G. In *Solid State Physics*; Liebert, L., Ed.; Academic Press: New York, 1978; Supplement 14, p 1.
- (14) Halperin, A.; Tirrell, M.; Lodge, T. P. *Adv. Polym. Sci.* **1992**, 100, 31.
- (15) Price, C. *Pure Appl. Chem.* **1983**, 55, 1563.
- (16) Price, C.; Chan, E. K. M.; Mobbs, R. H.; Stubbersfield, R. B. *Eur. Polym. J.* **1985**, 21, 355.
- (17) Price, C.; Chan, E. K. M.; Stubbersfield, R. B. *Eur. Polym. J.* **1987**, 23, 649.
- (18) Price, C.; Stubbersfield, R. B.; El-Kafrawy, S.; Kendall, K. D. *Br. Polym. J.* **1989**, 21, 391.
- (19) Deng, Y.; Price, C.; Booth, C. *Eur. Polym. J.* **1994**, 30, 103.
- (20) Quintana, J. R.; Villacampa, M.; Salazar, R.; Katime, I. A. *J. Chem. Soc., Faraday Trans.* **1992**, 88, 2793.
- (21) Quintana, J. R.; Villacampa, M.; Katime, I. A. *Macromolecules* **1993**, 26, 601.
- (22) Zhou, Z.; Chu, B.; Peiffer, D. G. *Macromolecules* **1993**, 26, 1876.
- (23) Zhou, Z.; Chu, B. *Macromolecules* **1994**, 27, 2025.
- (24) Zhou, Z.; Chu, B.; Peiffer, D. G. *Langmuir* **1995**, 11, 1956.
- (25) Quintana, J. R.; Janez, M. D.; Villacampa, M.; Katime, I. A. *Macromolecules* **1995**, 28, 4139.
- (26) Quintana, J. R.; Janez, M. D.; Katime, I. A. *Langmuir* **1996**, 12, 2196.
- (27) Alexandridis, P.; Holzwarth, J. F.; Hatton, T. A. *Macromolecules* **1994**, 27, 2414.
- (28) Alexandridis, P.; Nivaggioli, T.; Hatton, T. A. *Langmuir* **1995**, 11, 1468.
- (29) Alexandridis, P.; Athanassiou, V.; Hatton, T. A. *Langmuir* **1995**, 11, 2442.
- (30) Wilhelm, M.; Zhao, C. L.; Wang, Y.; Xu, R.; Winnik, M. A. *Macromolecules* **1991**, 24, 1033.
- (31) Deng, Y.; Yu, G. E.; Price, C.; Booth, C. *J. Chem. Soc., Faraday Trans.* **1992**, 88, 1441.
- (32) Alexandridis, P.; Hatton, T. A. *Colloids Surf. A* **1995**, 96, 1.
- (33) Price, C.; Chan, E. K. M.; Pilcher, G.; Stubbersfield, B. *Eur. Polym. J.* **1985**, 21, 627.
- (34) Wanka, G.; Hoffmann, H.; Ulbricht, W. *Colloid Polym. Sci.* **1990**, 268, 101. Wanka, G.; Hoffmann, H.; Ulbricht, W. *Macromolecules* **1994**, 27, 4145. Armstrong, J.; Chowdhry, B.; Mitchell, J.; Beezer, A.; Leharne, S. J. *Phys. Chem.* **1996**, 100, 1738.
- (35) Lindman, B.; Wennerstrom, H. In *Topics in Current Chemistry: Micelles*; Boschke, F. L., Ed.; Springer-Verlag: New York, 1980; p 34.
- (36) Hiemenz, P. C. *Principles of Colloid and Surface Chemistry*, 2nd ed.; Marcel Dekker: New York, 1986; p 447.
- (37) Hunter, R. J. *Foundations of Colloid Science*; Oxford University Press: New York, 1987; Vol. 1, p 575.
- (38) Zhong, X.-F.; Varshney, S. K.; Eisenberg, A. *Macromolecules* **1992**, 25, 7160.
- (39) Zhou, Z.; Chu, B. *Macromolecules* **1987**, 20, 3089. Zhou, Z.; Chu, B. **1988**, 21, 2548.
- (40) Kratochvil, P. In *Classical Light Scattering from Polymer Solutions*; Jenkins, A. D., Ed.; Elsevier Science Publisher: New York, 1987; p 115.
- (41) Mandema, W.; Emeis, C. A.; Zeldenrust, H. *Makromol. Chem.* **1979**, 180, 2163. Canham, P. A.; Lally, T. P.; Price, C.; Stubbersfield, R. B. *J. Chem. Soc., Faraday Trans. 1*, **1980**, 76, 1857. Sikora, A.; Tuzar, Z. *Makromol. Chem.* **1983**, 184, 2049. Price, C.; Briggs, N.; Quintana, J. R.; Stubbersfield, R. B.; Robb, I. *Polym. Commun.* **1986**, 27, 292.
- (42) Quintana, J. R.; Salazar, R. A.; Katime, I. A. *J. Phys. Chem.* **1995**, 99, 3723.
- (43) Barlow, R. J.; Zimmerman, S.; Khougaz, K.; Eisenberg, A. *J. Polym. Sci., Part B: Polym. Phys.* **1996**, 34, 1197.
- (44) Nagarajan, R.; Ganesh, K. *J. Chem. Phys.* **1989**, 90, 5843.
- (45) Tanford, C. *The Hydrophobic Effect: Formation of Micelles and Biological Membranes*, 2nd ed.; Wiley: New York, 1980; p 65.
- (46) The number of block units is calculated from the molecular weights provided in ref 17. The thermodynamic functions are copied from ref 17, and the standard states are ideal dilute solutions with unity molarity.
- (47) The ΔG°_{298K} values are calculated from the ΔH° and ΔS° values given in ref 29, where the standard states are ideal dilute solutions in unity mole fraction.
- (48) Callaghan, A.; Doyle, R.; Alexander, E.; Palepu, R. *Langmuir* **1993**, 9, 3422.